Journal of Solid State Chemistry 181 (2008) 2488–2493

Contents lists available at ScienceDirect

Journal of Solid State Chemistry

journal homepage: www.elsevier.com/locate/jssc

# Lanthanide complexes of the monovacant Dawson polyoxotungstate $[\alpha_2\text{-}As_2W_{17}O_{61}]^{10-}$ with 1D chain: Synthesis, structures, and photoluminescence properties

Xin-Yu Zhao [a], Shu-Xia Liu [a,*], Yuan-Hang Ren [a], Jian-Fang Cao [a], Rui-Ge Cao [a], Kui-Zhan Shao [b]

[a] Key Laboratory of Polyoxometalates Science of Ministry of Education, College of Chemistry, Northeast Normal University, Changchun City, 130024 Jilin, PR China
[b] Faculty of Chemistry, Institute of Functional Material Chemistry, Northeast Normal University, Changchun City, 130024 Jilin, PR China

ARTICLE INFO

*Article history:*
Received 1 March 2008
Received in revised form
10 May 2008
Accepted 24 May 2008
Available online 5 June 2008

*Keywords:*
Polyoxometalate
Tungstoarsenate
Lanthanide
Photoluminescence

ABSTRACT

Six new lanthanide complexes, $(H_3O)[Ln_3(H_2O)_{17}(\alpha_2\text{-}As_2W_{17}O_{61})]\cdot nH_2O$ ((**1**) $Ln = Ce^{III}$ and $n \approx 13$; (**2**) $Ln = Pr^{III}$ and $n \approx 9$; (**3**) $Ln = Nd^{III}$ and $n \approx 14$; (**4**) $Ln = Sm^{III}$ and $n \approx 8$; (**5**) $Ln = Eu^{III}$ and $n \approx 4$; (**6**) $Ln = Gd^{III}$ and $n \approx 7$), have been isolated by conventional solution method and characterized by elemental analysis, IR spectroscopy and single crystal X-ray diffraction. All the complexes are isomorphic and crystallize in the triclinic space group *P*-1. These complexes are 1D chain-like structures constructed by lanthanide cations and monovacant Dawson-type $[\alpha_2\text{-}As_2W_{17}O_{61}]^{10-}$ polyoxoanions. The striking feature of the structures is that there are three kinds of coordination environments for lanthanide cations, which are responsible for the formation of polymeric structures. Photoluminescence measurements reveal that **4** and **5** exhibit orange and red fluorescent emission at room temperature, respectively.



## 1. Introduction

Polyoxometalates (POMs) are polymetallic cluster compounds presenting a very large diversity of structures [1]. They exhibit many properties that make them attractive for applications in different fields including catalysis, medicine and materials science [2]. Because of their multiple coordination requirements and high oxophilic activities, lanthanide (*Ln*) ions are suitable for linking POM building blocks to form new classes of materials with extended metal–oxygen frameworks. More specifically, lanthanides can impart useful functionality such as luminescence [3], magnetism [4], and Lewis acid catalytic centers [5] to POMs, which extend their range of physical and chemical properties of the resulting complexes.

During the last two decades, many efforts have been explored on the construction of lanthanopolyoxometalates. In reported work, lanthanide cations link POMs, such as Anderson [6], Silverton-type [7], $[MV_{13}O_{38}]^{7-}$ ($M$ = Mn, Ni) [8], and some nano-sized polyoxoanions [9], by binding to surface terminal or bridging oxygen atoms to form multidimensional assemblies. Lanthanide cations also incorporate with the basic oxygen atoms at a defect site in lacunary POMs. Typical examples are the monovacant Keggin or Dawson-type polyoxoanions form both 1:1 and 1:2 complexes with lanthanide cations, while these structures are discrete anions [10,11]. In 2000, Pope et al. investigated the structural characterization of the one-dimensional 1:1 $[Ln(\alpha\text{-}SiW_{11}O_{39})(H_2O)_3]^{5-}$ ($Ln = La^{III}$ and $Ce^{III}$) complexes [12], and showed that these polyoxoanions are polymeric in the solid state. Then, lanthanide cations/monovacant Keggin-type polyoxoanions system has been the subject of a lot of papers [13]. In contrast, studies on classical monovacant Dawson-type polyoxoanions are still in their infancy. It is quite appealing and challenging to prepare lanthanopolyoxometalates based on monovacant Dawson-type building block with extended framework. A reported work on $[Ln(H_2O)_2(\alpha_2\text{-}P_2W_{17}O_{61})]_n^{7n-}$, which displays 1D chain-like structure, suggested that the monovacant Dawson-type building block was a good precursor, and the proper reaction conditions turned out to be a good way to introduce lanthanide cations in different coordination ways [14]. We attempted to make use of monovacant Dawson-type $[\alpha_2\text{-}As_2W_{17}O_{61}]^{10-}$ polyoxoanions as building blocks to realize the molecular assemblies with lanthanide cations. To the best of our knowledge, only three examples for $Ln^{3+}$ ions incorporated monovacant Dawson-type tungstoarsenates which are the 1:2-type dimers, $[Ln(As_2W_{17}O_{61})_2]^{17-}$ [15].

In this paper, we investigate the solution reaction of $[\alpha_2\text{-}As_2W_{17}O_{61})]^{10-}$ polyoxoanions with $Ln^{3+}$ ions, and successfully obtained six isomorphic lanthanide complexes, $(H_3O)[Ln_3(H_2O)_{17}(\alpha_2\text{-}As_2W_{17}O_{61})]\cdot nH_2O$ ((**1**) $Ln = Ce^{III}$ and $n \approx 13$; (**2**) $Ln = Pr^{III}$ and $n \approx 9$; (**3**) $Ln = Nd^{III}$ and $n \approx 14$; (**4**) $Ln = Sm^{III}$ and $n \approx 8$;

* Corresponding author. Fax.: +86 431 85099328.
*E-mail address:* liusx@nenu.edu.cn (S.-X. Liu).

0022-4596/$ - see front matter © 2008 Elsevier Inc. All rights reserved.
doi:10.1016/j.jssc.2008.05.044

(**5**) $Ln = Eu^{III}$ and $n \approx 4$; (**6**) $Ln = Gd^{III}$ and $n \approx 7$). These complexes exhibit the example of lacunary Dawson-type polyoxoanions incorporating lanthanide cations, and lanthanide cations acting as an effective bridge to link discrete dimmers. It is the first *Ln*-containing tungstoarsenate with extended structures. Here, the syntheses and structures are reported, and the luminescence properties of the relative $Eu^{III}$ and $Sm^{III}$ complexes are presented as well.

## 2. Experimental section

### 2.1. General methods and materials

The $K_6[\alpha\text{-}As_2W_{18}O_{62}] \cdot 14H_2O$ was prepared according to the literature [16] and confirmed by IR spectroscopy. The $Eu(ClO_4)_3 \cdot xH_2O$ ($x \approx 6$–8) was prepared by the reaction of $Eu_2O_3$ and $HClO_4$. Other reagents were used as purchased without further purification. Elemental analyses (Ce, Pr, Nd, Sm, Eu, Gd, As, and W) were performed on a PLASMA-SPEC(I) ICP atomic emission spectrometer. IR spectra were recorded in the range 400–4000 $cm^{-1}$ on an Alpha Centaurt FT/IR spectrophotometer using KBr pellets. TG analysis was performed on a Perkin-Elmer TGA7 instrument in $N_2$ atmosphere with a heating rate of 10 °C $min^{-1}$. Photoluminescence measurements were carried out on a Hitachi F-4500 Fluorescence Spectrophotometer.

### 2.2. Synthesis of $(H_3O)[Ce_3(H_2O)_{17}(\alpha_2\text{-}As_2W_{17}O_{61})] \cdot \sim 13H_2O$ **1**

$K_6[\alpha\text{-}As_2W_{18}O_{62}] \cdot 14H_2O$ (0.59 g, 0.12 mmol) and $LiClO_4 \cdot 3H_2O$ (0.96 g, 6 mmol) were dissolved in 20 mL of water and the solution was stirred for 5 min, then pH was adjusted to 6.5 by the addition of $Na_2CO_3$ and the mixture was heated to 80 °C. After that, 10 mL of water solution of $Ce(NO_3)_3 \cdot 6H_2O$ (0.31 g, 0.72 mmol) was added. The resulting cloudy solution was refluxed at 80 °C and stirred for 1 h, and then filtered. The filtrate was kept for 5 days at room temperature for crystallization. Orange block crystals of **1** were collected. Yield: 58% (based on W). Elemental anal. Calcd. for **1** (%): Ce, 8.04; As, 2.86; W, 59.75. Found (%): Ce, 7.90; As, 2.82; W, 59.30. The selected IR (KBr pellet, $cm^{-1}$): 3413(m), 954(m), 862(s), 825(s), 779(s), 521(m).

### 2.3. Synthesis of $(H_3O)[Pr_3(H_2O)_{17}(\alpha_2\text{-}As_2W_{17}O_{61})] \cdot \sim 9H_2O$ **2**

Complex **2** was prepared following the procedure described for complex **1**, but $PrCl_3 \cdot 6H_2O$ was used instead of $Ce(NO_3)_3 \cdot 6H_2O$. Yield: 62% (based on W). Elemental anal. Calcd. for **2** (%): Pr, 8.19; As, 2.90; W, 60.55. Found (%): Pr, 8.10; As, 2.83; W, 60.08. The selected IR (KBr pellet, $cm^{-1}$): 3403(m), 954(m), 862(s), 823(s), 780(s), 522(m).

### 2.4. Synthesis of $(H_3O)[Nd_3(H_2O)_{17}(\alpha_2\text{-}As_2W_{17}O_{61})] \cdot \sim 14H_2O$ **3**

Complex **3** was prepared following the procedure described for complex **1**, but $NdCl_3 \cdot 6H_2O$ was used instead of $Ce(NO_3)_3 \cdot 6H_2O$. Yield: 70% (based on W). Elemental anal. Calcd. for **3** (%): Nd, 8.22; As, 2.85; W, 59.40. Found (%): Nd, 8.13; As, 2.79; W, 59.00. The selected IR (KBr pellet, $cm^{-1}$): 3414(m), 955(m), 863(s), 824(s), 781(s), 523(m).

### 2.5. Synthesis of $(H_3O)[Sm_3(H_2O)_{17}(\alpha_2\text{-}As_2W_{17}O_{61})] \cdot \sim 8H_2O$ **4**

Complex **4** was prepared following the procedure described for complex **1**, but $SmCl_3 \cdot 6H_2O$ was used instead of $Ce(NO_3)_3 \cdot 6H_2O$. Yield: 54% (based on W). Elemental anal. Calcd. for **4** (%): Sm, 8.72; As, 2.90; W, 60.43. Found (%): Sm, 8.62; As, 2.84; W, 59.98. The selected IR (KBr pellet, $cm^{-1}$): 3403(m), 956(m), 863(s), 825(s), 780(s), 522(m).

### 2.6. Synthesis of $(H_3O)[Eu_3(H_2O)_{17}(\alpha_2\text{-}As_2W_{17}O_{61})] \cdot \sim 4H_2O$ **5**

Complex **5** was prepared following the procedure described for complex **1**, but $Eu(ClO_4)_3 \cdot xH_2O$ was used instead of $Ce(NO_3)_3 \cdot 6H_2O$. Yield: 50% (based on W). Elemental anal. Calcd. for **5** (%): Eu, 8.93; As, 2.94; W, 61.23. Found (%): Eu, 8.83; As, 2.89; W, 60.75. The selected IR (KBr pellet, $cm^{-1}$): 3414(m), 956(m), 864(s), 823(s), 779(s), 523(m).

### 2.7. Synthesis of $(H_3o)[Gd_3(H_2O)_{17}(\alpha_2\text{-}As_2W_{17}O_{61})] \cdot \sim 7H_2O$ **6**

Complex **6** was prepared following the procedure described for complex **1**, but $GdCl_3 \cdot 6H_2O$ was used instead of $Ce(NO_3)_3 \cdot 6H_2O$. Yield: 55% (based on W). Elemental anal. Calcd. for **6** (%): Gd, 9.11; As, 2.89; W, 60.40. Found (%): Gd, 9.00; As, 2.84; W, 59.98. The selected IR (KBr pellet, $cm^{-1}$): 3414(m), 957(m), 864(s), 824(s), 780(s), 521(m).

### 2.8. X-ray crystallography

Diffraction intensities for complexes **1**–**6** were collected on a Siemens SMART-CCD with Mo-$K\alpha$ monochromated radiation ($\lambda = 0.71073$ Å) at 293 K. The linear absorption coefficients, scattering factors for the atoms, and the anomalous dispersion corrections were taken from International Tables for X-ray Crystallography. The structures were solved by direct methods and refined by the full-matrix least-squares method on $F^2$ using the SHELXTL crystallographic software package. Empirical absorption corrections were applied. Anisotropic thermal parameters were used to refine all nonhydrogen atoms. All the hydrogen atoms for water molecules and protonation were not located but were included in the structure factor calculations. Inside the frameworks of all the compounds, there are a number of disordered lattice water molecules, which show many peaks of low electronic density in the difference Fourier maps. So the SQUEEZE subroutine of PLATON software [17] was applied to create new reflection data in which contributions from the disordered lattice waters were removed from the original data. The crystal data and structure refinements of complexes **1**–**6** on the basis of the new reflection data were summarized in Table 1. The number of lattice water molecules for **1**–**6** are determined by thermal gravimetric (TG) analyses (Fig. S5). Further details of the crystal structure investigations of **1**–**6** may be obtained from the Fachinformationszentrum Karlsruhe, D-76344 Eggenstein-Leopoldshafen, Germany (E-mail: Crysdata@fiz-karlstruhe.de) on quoting the deposited numbers, which are CSD-417528, CSD-417527, CSD-417529, CSD-417526, CSD-417525 and CSD-417993, respectively.

## 3. Results and discussion

### 3.1. Synthesis

Six lanthanide complexes were successfully prepared using the similar synthetic procedure by reaction of the respective lanthanide cations with the monovacant $[\alpha_2\text{-}As_2W_{17}O_{61}]^{10-}$ polyoxoanions. The $[\alpha_2\text{-}As_2W_{17}O_{61}]^{10-}$ polyoxoanions were freshly prepared by adjustment of the pH of the solution of $[\alpha_2\text{-}As_2W_{18}O_{62}]^{6-}$ to 6.5 through the addition of $Na_2CO_3$. It is noted that there is a competition between the $K^+$ and $Ln^{3+}$ ions in

**Table 1**
Crystal data and structure refinements for **1**–**6**

| | **1** | **2** | **3** | **4** | **5** | **6** |
|---|---|---|---|---|---|---|
| Empirical | $H_{63}Ce_3O_{92}$ | $H_{55}Pr_3O_{88}$ | $H_{65}Nd_3O_{93}$ | $H_{53}Sm_3O_{87}$ | $H_{45}Eu_3O_{83}$ | $H_{51}Gd_3O_{86}$ |
| Formula | $As_2W_{17}$ | $As_2W_{17}$ | $As_2W_{17}$ | $As_2W_{17}$ | $As_2W_{17}$ | $As_2W_{17}$ |
| fw | 5231.15 | 5161.46 | 5261.53 | 5171.76 | 5104.53 | 5174.45 |
| Cryst syst | Triclinic | Triclinic | Triclinic | Triclinic | Triclinic | Triclinic |
| Space group | *P*-1 | *P*-1 | *P*-1 | *P*-1 | *P*-1 | *P*-1 |
| *a* (Å) | 14.4927(12) | 14.3937(19) | 14.4292(7) | 14.249(2) | 14.1735(9) | 14.2515(7) |
| *b* (Å) | 17.4089(15) | 17.386(2) | 17.4287(8) | 17.368(3) | 17.4134(11) | 17.4471(9) |
| *c* (Å) | 20.0329(16) | 19.980(3) | 19.9900(10) | 19.878(3) | 19.8716(13) | 19.9028(10) |
| $\alpha$ (deg) | 82.885(2) | 82.882(3) | 82.8620(10) | 82.980(3) | 83.1330(10) | 83.0720(10) |
| $\beta$ (deg) | 72.496(2) | 72.605(3) | 72.5270(10) | 72.997(3) | 73.2070(10) | 72.8040(10) |
| $\gamma$ (deg) | 77.995(2) | 77.962(3) | 77.9580(10) | 77.947(3) | 78.0660(10) | 78.0730(10) |
| *V* (Å$^3$) | 4704.7(7) | 4656.2(11) | 4679.4(4) | 4590.6(11) | 4584.5(5) | 4616.1(4) |
| *Z* | 2 | 2 | 2 | 2 | 2 | 2 |
| *Dc* (g cm$^{-3}$) | 3.693 | 3.681 | 3.734 | 3.742 | 3.698 | 3.723 |
| $\mu$ (mm$^{-1}$) | 22.912 | 23.248 | 23.242 | 23.906 | 24.062 | 24.019 |
| *F* (000) | 4594 | 4520 | 4626 | 4518 | 4444 | 4510 |
| $\theta$ range (deg) | 1.07–25.50 | 1.07–26.15 | 1.55–26.15 | 1.07–25.50 | 1.07–25.50 | 1.07–26.00 |
| GOF on $F^2$ | 0.931 | 0.924 | 0.934 | 0.939 | 0.918 | 0.962 |
| $R_1$ [$I>2\sigma(I)$][a] | 0.0527 | 0.0580 | 0.0447 | 0.0782 | 0.0572 | 0.0507 |
| w$R_2$ [$I>2\sigma(I)$][a] | 0.1180 | 0.1329 | 0.0979 | 0.1934 | 0.1242 | 0.1113 |
| $R_1$ (all data)[b] | 0.0787 | 0.0892 | 0.0684 | 0.1092 | 0.0911 | 0.0737 |
| w$R_2$ (all data)[b] | 0.1284 | 0.1470 | 0.1056 | 0.2092 | 0.1357 | 0.1196 |

[a] $R_1 = \Sigma||Fo|-|Fc||/\Sigma|Fo|$.
[b] $wR_2 = [\Sigma w(Fo^2-Fc^2)^2/\Sigma w(Fo^2)^2]^{1/2}$.

our reaction system due to the similarity of ionic radii (radii: $K^+ = 133$ pm; $Ln^{3+} = 106$–98.5 pm), and oxophilicity. Especially, they both present the similar coordination requirements. Furthermore, the examples of $K^+$ ions as linker in POM complexes have been observed in the previous work [6c,10c,18,19]. To introduce lanthanide cations to act as effective linkers and avoid the interference of $K^+$ ions, we use $ClO_4^-$ ions to eliminate the $K^+$ ions during the preparation of these complexes.

### 3.2. Crystal structures

Single crystal X-ray diffraction analyses reveal that complexes **1**–**6** are isomorphic and the related bond distances, angles and the number of lattice waters vary only slightly. The solid-state structures of complexes **1**–**6** consist of infinite 1D chain-like arrangement built up of monovacant $[\alpha_2\text{-}As_2W_{17}O_{61}]^{10-}$ polyoxoanions and trivalent lanthanide cations. The $[\alpha_2\text{-}As_2W_{17}O_{61}]^{10-}$ polyoxoanion is obtained by base degradation of the parent Dawson polyoxoanion: effectively, removal of a $[WO]^{4+}$ unit from a "cap" $WO_6$ polyhedron of the parent $[\alpha\text{-}As_2W_{18}O_{62}]^{6-}$. In complexes **1**–**6**, the As–O bond distances vary between 1.642(11) and 1.735(18) Å, and the O–As–O bond angles vary between 105.0(9)° and 113.1(8)°. The W–O bond distances are in the range of 1.666(17)–2.366(12) Å. The O–W–$O_{cis}$ and O–W–$O_{trans}$ bond angles are within 69.2(5)–107.1(9)° and 152.0(8)–175.4(7)°, respectively.

The structure of **1** is shown in Fig. 1. The Ce(1) cation occupies the vacant site of a $[\alpha_2\text{-}As_2W_{17}O_{61}]^{10-}$ subunit and is coordinated to the four oxygen atoms of the vacant site ($d_{Ce(1)-O}$ = 2.398(13)–2.460(10) Å), three water molecules ($d_{Ce(1)-OH2}$ = 2.517(14)–2.570(16) Å), and a terminal oxygen atom of another $[\alpha_2\text{-}As_2W_{17}O_{61}]^{10-}$ subunit ($d_{Ce(1)-Od}$ = 2.500(11) Å). It is interesting that two Ce(1) centers connect two $[\alpha_2\text{-}As_2W_{17}O_{61}]^{10-}$ subunits via two terminal oxygen atoms to form a dimeric cluster. A polyhedral structure is shown in Fig. 2a. Each Ce(1) atom is in a distorted square antiprismatic coordination geometry (Fig. 3). Further studies reveal that each dimeric $[Ce_2(H_2O)_6(\alpha_2\text{-}As_2W_{17}O_{61})_2]^{14-}$ anion acts as a tetradentate ligand coordinating

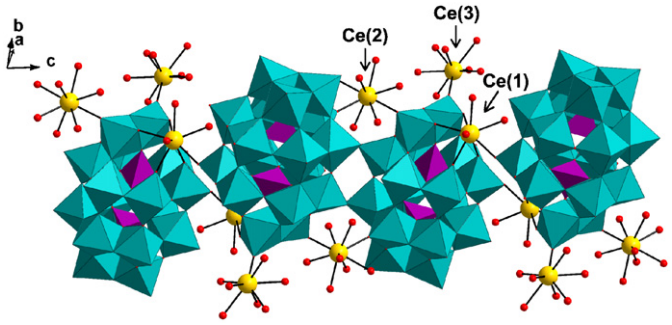


**Fig. 1.** Polyhedral view of the 1D chain in **1**. The $AsO_4$ and $WO_6$ polyhedra are shown in violet and teal, respectively. The Ce1, Ce2, and Ce3 atoms are shown as a gold ball. Their coordinational water molecules are shown as a red ball. Crystallization water molecules have been omitted.

four Ce(2) centers via four terminal oxygen atoms of tungsten ($d_{Ce(2)-Od}$ = 2.491(10)–2.564(12) Å) (Fig. 2b). Through the linkage of Ce(2) atoms, the dimeric cluster form 1D chain-like structure running along the *b*-axis (Fig. S2). Each Ce(2) atom has a coordination number of nine and resides in the center of a distorted tricapped trigonal prism (Fig. 3). The coordination oxygen atoms around the Ce(2) atom contain two terminal oxygen atoms of tungsten, and seven oxygen atoms from water molecules ($d_{Ce(2)-OH2}$ = 2.493(15)–2.61(12) Å). An additional feature is that Ce(3) center connects each $[\alpha_2\text{-}As_2W_{17}O_{61}]^{10-}$ subunit via terminal oxygen atom (terminal W = O oxygen atoms are attributed to "cap" triple with removal of a $[WO]^{4+}$ unit) to incorporate the 1D chain-like structure (Fig. S3). The Ce(3) atom is also of eight coordinates with a distorted square antiprism environment (Fig. 3), defined by eight coordination oxygen atoms, seven from water molecules ($d_{Ce(3)-OH2}$ = 2.45(3)–2.65(4) Å) and one from the $[\alpha_2\text{-}As_2W_{17}O_{61}]^{10-}$ subunits ($d_{Ce(3)-Od}$ = 2.457(12) Å). In the reported work, the monovacant Dawson polyoxoanions $[\alpha_2\text{-}As_2W_{17}O_{61}]^{10-}$ are linked together only by the $Ln^{3+}$ ions coordinated to the vacant sites [15]. However, in complex **1**, the monovacant Dawson polyoxoanions are linked alternately by the

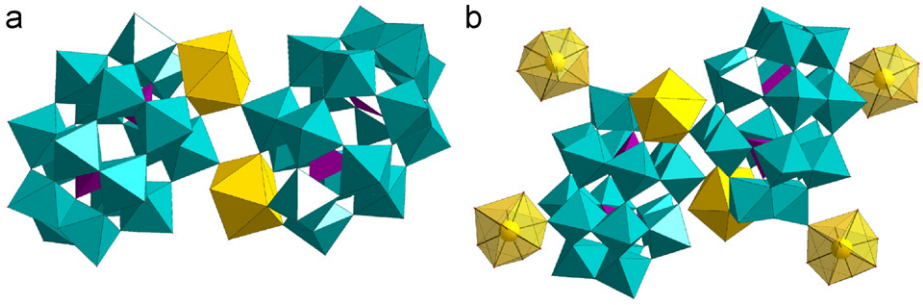


**Fig. 2.** (a) Polyhedral representation of the dimeric $\{Ce(H_2O)_3(\alpha_2\text{-}As_2W_{17}O_{61})\}_2$. $\{Ce(1)(H_2O)_3\}$ fragments in gold polyhedral representation. (b) Polyhedral representation of the building block unit in **1**. The dimeric is the same as in (a). $\{Ce(2)(H_2O)_7\}$ fragments in gold polyhedral representation with translucency.

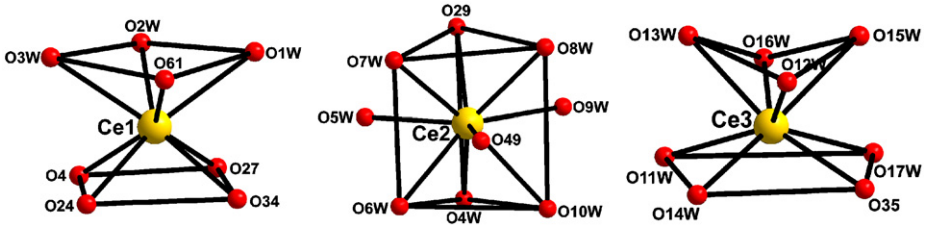


**Fig. 3.** The coordination environment of Ce1, Ce2, and Ce3 in complex **1**.

$Ce^{3+}$ ion coordinated to the vacant sites and discrete $Ce^{3+}$ ion linkers.

This reported work suggested that the effective radius of the central element ($As^{5+}$, 0.46 Å and $P^{5+}$, 0.35 Å) has no significant effect on the surrounding metal–oxo framework. But compared with the isomorphic monovacant species $[\alpha_2\text{-}P_2W_{17}O_{61}]^{10-}$, the polyoxoanion $[\alpha_2\text{-}As_2W_{17}O_{61}]^{10-}$ contains the larger "bite angle". So $[\alpha_2\text{-}As_2W_{17}O_{61}]^{10-}$ may allow the rare earth cation to bind deeper into the defect site. In the isomorphic anions $[Nd(H_2O)_3(\alpha_2\text{-}As_2W_{17}O_{61})]^{7-}$ and $[Nd(H_2O)_3(\alpha_2\text{-}P_2W_{17}O_{61})]^{7-}$ [10d], the As–Nd distance (4.417 Å) is shorter than the P–Nd distance (4.423 Å). In addition, the aperture of the vacant site in $[\alpha_2\text{–}As_2W_{17}O_{61}]^{10-}$ ($d_{O20\text{–}O13} = 4.160$ Å) is larger than that of the $[\alpha_2\text{-}P_2W_{17}O_{61}]^{10-}$ ($d_{O18\text{–}O17} = 4.119$ Å) (Fig. S4).

The bond-valence calculations [20] suggest that in **1**, all As atoms are in the +5 oxidation state, all W atoms are in the +6 oxidation state, and the Ce sites are in the +3 oxidation state. The difference Fourier map reveals that no $K^+$ ion is present, which is further confirmed by elemental analyses. The negative charge retained in the structure of **1** is compensated by the protonation of a lattice water molecule. Consequently, the formula of **1** is regarded as $(H_3O)[Ce_3(H_2O)_{17}(\alpha_2\text{-}As_2W_{17}O_{61})]\cdot\sim 13H_2O$. Similar results have also been obtained for complexes **2**–**6**.

### 3.3. FT-IR spectroscopy

The IR spectra of complexes **1**–**6** are very similar and show the characteristic asymmetric vibration patterns of the Dawson-type polyoxoanion in the low-wavenumber region ($\nu < 1000$ $cm^{-1}$). In comparison with the parent Dawson polyoxoanion $[\alpha\text{-}As_2W_{18}O_{62}]^{6-}$ (see Table 2 and Fig. 4), the $\nu_{as}(W\text{–}O_d)$ vibration frequencies (954–956 $cm^{-1}$) have red shifts of 15–17 $cm^{-1}$; the major reason may be that the rare earth cations have stronger interactions to the terminal oxygen atoms of the polyoxoanions, impairing the $W\text{–}O_d$ bond, reducing the $W\text{–}O_d$ bond force constant, leading to a decrease in the $W\text{–}O_d$ vibration frequency.

**Table 2**
IR spectra ($cm^{-1}$) of polyanions **1**-**6** and compared with the $K_6[\alpha\text{-}As_2W_{18}O_{62}]\cdot 14H_2O$

| Complex | $\nu_{as}(W\text{–}O_d)$ | $\nu_{as}(W\text{–}O_b)$ | $\nu_{as}(As\text{–}O_a)$ | $\nu_{as}(W\text{–}O_c)$ |
|---|---|---|---|---|
| $K_6[\alpha\text{-}As_2W_{18}O_{62}]\cdot 14H_2O$ | 971 | 891 | 865, 827 | 757 |
| $[Ce_3(H_2O)_{17}(\alpha_2\text{-}As_2W_{17}O_{61})]^-$ | 954 | 862 | 825 | 779, 692 |
| $[Pr_3(H_2O)_{17}(\alpha_2\text{-}As_2W_{17}O_{61})]^-$ | 954 | 862 | 823 | 780, 696 |
| $[Nd_3(H_2O)_{17}(\alpha_2\text{-}As_2W_{17}O_{61})]^-$ | 955 | 863 | 824 | 781, 694 |
| $[Sm_3(H_2O)_{17}(\alpha_2\text{-}As_2W_{17}O_{61})]^-$ | 956 | 863 | 825 | 780, 696 |
| $[Eu_3(H_2O)_{17}(\alpha_2\text{-}As_2W_{17}O_{61})]^-$ | 956 | 864 | 823 | 779, 691 |
| $[Gd_3(H_2O)_{17}(\alpha_2\text{-}As_2W_{17}O_{61})]^-$ | 957 | 864 | 824 | 780, 695 |

The $\nu_{as}(W\text{–}O_b)$ vibration frequencies (862–864 $cm^{-1}$) have red shifts of 28–30 $cm^{-1}$. As for $\nu_{as}(As\text{–}O_a)$, only one strong absorption peak at 825 $cm^{-1}$ could be clearly observed, which is almost equal to that of the parent $[\alpha\text{-}As_2W_{18}O_{62}]^{6-}$, but the other peak at 865 $cm^{-1}$ is overlapped by the strong peak of $\nu_{as}(W\text{–}O_b)$ at 862 $cm^{-1}$. The $\nu_{as}(W\text{–}O_c)$ peak splits into two peaks because of their lower symmetry compared to that of the parent $[\alpha\text{-}As_2W_{18}O_{62}]^{6-}$ ($D_{3h}$), by removing a $[WO]^{4+}$ unit.

### 3.4. Photoluminescence properties

Photoluminescence spectra of powder samples of complexes **4** and **5** have been measured at room temperature. As shown in Fig. 5a, the emission spectrum of **5** exhibits five characteristic transitions of the $Eu^{3+}$ ion under the excitation wavelength (397 nm). These peaks are assigned to five energy level transitions from $^5D_0$ metastable state to terminal levels, respectively: $^7F_J$ ($J = 0, 1, 2, 3, 4$) transitions. More clearly, the symmetric forbidden emission $^5D_0 \rightarrow {}^7F_0$ at 579 nm can be found, which reveals that $Eu^{3+}$ occupies a site with low symmetry and without an inversion center. The $^5D_0 \rightarrow {}^7F_1$ transition is the magnetic dipole transition, and its intensity is largely independent of the local environment of the europium ion. On the other hand, the $^5D_0 \rightarrow {}^7F_2$

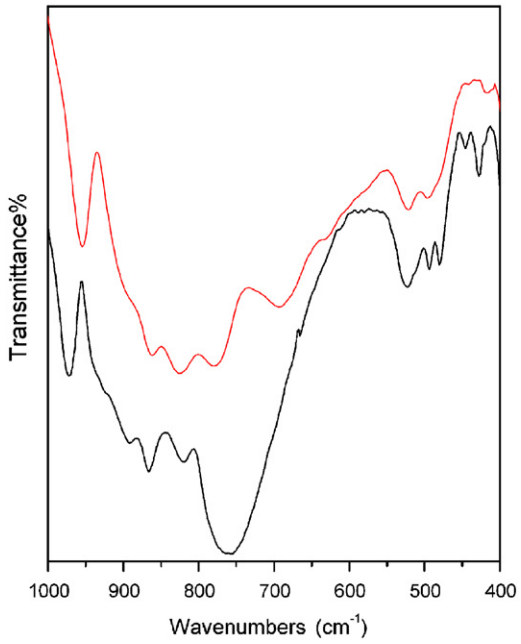


**Fig. 4.** IR spectra of $K_6[\alpha\text{-}As_2W_{18}O_{62}]\cdot 14H_2O$ and complex **1** are shown as the black and red lines, respectively.

transition is the electric dipole transition and is extremely sensitive to chemical bonds in the vicinity of $Eu^{3+}$, which increases as the site symmetry of $Eu^{3+}$ decreases. The $I(^5D_0\rightarrow{}^7F_2)/I(^5D_0\rightarrow{}^7F_1)$ ratio is widely used as a measure of the coordination state and the site symmetry of the rare earth [3,21]. For complex **5**, the strongest emission is in the $^5D_0\rightarrow{}^7F_2$ transition region with the $^5D_0\rightarrow{}^7F_2$ peak at 615 nm, while, the $^5D_0\rightarrow{}^7F_1$ transition is the next with the emission peak is at 591 nm. The intensity ratio $I(^5D_0\rightarrow{}^7F_2)/I(^5D_0\rightarrow{}^7F_1)$ is equal to 2.5, which also indicates that the symmetry of the $Eu^{3+}$ ion is low. This result is consistent with the coordination environment of the $Eu^{3+}$ ion in complex **5**. The intense $^5D_0\rightarrow{}^7F_2$ transition points to a highly polarizable chemical environment around the $Eu^{3+}$ ion that is responsible for the red emission of **5**.

Fig. 5b shows the emission spectrum of complex **4**, and the relatively intense luminescence arises from the intraconfigurational $^4G_{5/2}\rightarrow{}^6H_J$ transitions ($J = 5/2$, 7/2, and 9/2); the emission spectrum of **4** shows three characteristic transitions of the $Sm^{3+}$ ion under the excitation wavelength (405 nm). The peaks at 559, 595, 641 nm are attributed to the $^4G_{5/2}\rightarrow{}^6H_{5/2}$ (zero–zero band), $^4G_{5/2}\rightarrow{}^6H_{7/2}$ (magnetic dipole transition), and $^4G_{5/2}\rightarrow{}^6H_{9/2}$ (electronic dipole transition), respectively. It is shown that the magnetic dipole transition was the relatively stronger emission, which is responsible for the orange emission of **4**. Herein, the luminescent information on Sm-contained tungstoarsenates has been provided, which was described rarely. It may be attributed to the structure feature or the content of Sm in polymer.

## 4. Conclusions

In summary, six 1D chain-like lanthanide complexes constructed by lanthanide cations and monovacant Dawson-type anions $[\alpha_2\text{-}As_2W_{17}O_{61}]^{10-}$ have been synthesized by conventional solution method. The successful preparation of **1**–**6** demonstrates that the synthetic route using $ClO_4^-$ ions to eliminate $K^+$ ions may be powerful for the formation of extended structure by introducing *Ln* cations as linker. This work provides some luminescent information on lanthanide-contained monovacant Dawson-type tungstoarsenates, especially for the complex containing Sm.

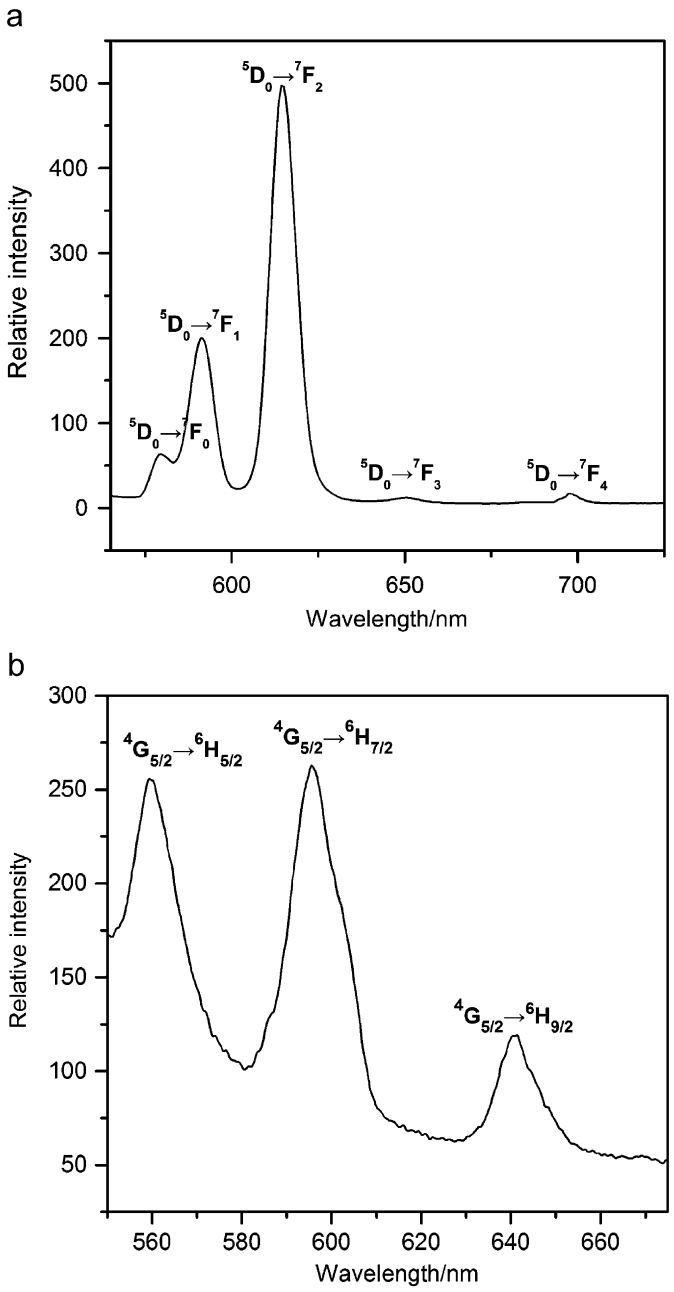


**Fig. 5.** Emission spectrum of solid **5** ($\lambda_{ex} = 397$ nm) (a) and **4** ($\lambda_{ex} = 405$ nm) (b).

## Acknowledgment

This work was supported by the National Science Foundation of China (Grant no. 20571014), the Program for New Century Excellent Talents in University (NCET–07–0169), and the Analysis and Testing Foundation of Northeast Normal University.

## Appendix A. Supplementary materials

The online version of this article contains additional supplementary data. Please visit doi:10.1016/j.jssc.2008.05.044.

## References


[1] (a) M.T. Pope, Heteropoly and Isopoly Oxometalates, Springer, Berlin, 1983;
(b) M.T. Pope, A. Müller, Angew. Chem. Int. Ed. Engl. 30 (1991) 34–48.
[2] (a) N. Mizuno, M. Misono, Chem. Rev. 98 (1998) 199–277;
(b) J.T. Rhule, C.L. Hill, D.A. Judd, Chem. Rev. 98 (1998) 327–357;
(c) E. Coronado, C.J. Gómez-García, Chem. Rev. 98 (1998) 273–296.
[3] T. Yamase, Chem. Rev. 98 (1998) 307–325.
[4] C. Benelli, D. Gatteschi, Chem. Rev. 102 (2002) 2369–2388.
[5] G. Molander, Chem. Rev. 92 (1992) 29–68.
[6] (a) B. Gao, S.X. Liu, L.H. Xie, M. Yu, C.D. Zhang, C.Y. Sun, J. Solid State Chem. 179 (2006) 1681–1689;
(b) R.G. Cao, S.X. Liu, L.H. Xie, Y.B. Pan, J.F. Cao, Y. Liu, Inorg. Chim. Acta 361 (2008) 2013–2018;
(c) V. Shivaiah, P.V.N. Reddy, L. Cronin, S.K. Das, Dalton Trans. (2002) 3781–3782;
(d) D. Drewes, E.M. Limanski, B. Krebs, Dalton Trans. (2004) 2087–2091;
(e) D. Drewes, E.M. Limanski, B. Krebs, Eur. J. Inorg. Chem. (2004) 4849–4853.
[7] C.D. Wu, C.Z. Lu, H.H. Zhuang, J.S. Huang, J. Am. Chem. Soc. 124 (2002) 3836–3837.
[8] S.X. Liu, D.H. Li, L.H. Xie, H.Y. Cheng, X.Y. Zhao, Inorg. Chem. 45 (2006) 8036–8040.
[9] (a) N.V. Izarova, M.N. Sokolov, D.G. Samsonenko, A. Rothenberger, D.Y. Naumov, D. Fenske, V.P. Fedin, Eur. J. Inorg. Chem. (2005) 4985–4996;
(b) M. Zimmermann, N. Belai, R.J. Butcher, M.T. Pope, E.V. Chubarova, M.H. Dickman, U. Kortz, Inorg. Chem. 46 (2007) 1737–1740.
[10] (a) R.D. Peacock, T.J.R. Weakley, J. Chem. Soc. A. (1971) 1836–1839;
(b) R. Copping, A.J. Gaunt, I. May, M.J. Sarsfield, D. Collison, M. Helliwell, I.S. Denniss, D.C. Apperley, Dalton Trans. (2005) 1256–1262;
(c) B.S. Bassil, M.H. Dickman, B. Kammer, U. Kortz, Inorg. Chem. 46 (2007) 2452–2458;
(d) O.A. Kholdeeva, M.N. Timofeeva, G.M. Maksimov, R.I. Maksimovskaya, W.A. Neiwert, C.L. Hill, Inorg. Chem. 44 (2005) 666–672;
(e) A.J. Gaunt, I. May, M.J. Sarsfield, D. Collison, M. Helliwell, I.S. Denniss, Dalton Trans. (2003) 2767–2771.
[11] (a) Q.H. Luo, R.C. Howell, M. Dankova, J. Bartis, C.W. Williams, W.D. Horrocks Jr., V.G. Young Jr., A.L. Rheingold, L.C. Francesconi, M.R. Antonio, Inorg. Chem. 40 (2001) 1894–1901;
(b) Q.H. Luo, R.C. Howell, J. Bartis, M. Dankova, W.D. Horrocks Jr., A.L. Rheingold, L.C. Francesconi, Inorg. Chem. 41 (2002) 6112–6117;
(c) M. Sadakane, M.H. Dickman, M.T. Pope, Inorg. Chem. 40 (2001) 2715–2719;
(d) C. Boglio, G. Lemière, B. Hasenknopf, S. Thorimbert, E. Lacôte, M. Malacria, Angew. Chem. Int. Ed. 45 (2006) 3324–3327.
[12] M. Sadakane, M.H. Dickman, M.T. Pope, Angew. Chem. Int. Ed. 39 (2000) 2914–2916.
[13] (a) P. Mialane, L. Lisnard, A. Mallard, J. Marrot, E. Antic-Fidancev, P. Aschehoug, D. Vivien, F. Sécheresse, Inorg. Chem. 42 (2003) 2102–2108;
(b) J.P. Wang, X.Y. Duan, X.D. Du, J.Y. Niu, Cryst. Growth Des. 6 (2006) 2266–2270;
(c) J.P. Wang, J.W. Zhao, X.Y. Duan, J.Y. Niu, Cryst. Growth Des. 6 (2006) 507–513;
(d) F.L. Sousa, F.A.A. Paz, C.M.C.E. Granadeiro, A.M.V. Cavaleiro, J. Rocha, J. Klinowski, H.I.S. Nogueira, Inorg. Chem. Commun. 8 (2005) 924–927.
[14] Y. Lu, Y. Xu, Y.G. Li, E.B. Wang, X.X. Xu, Y. Ma, Inorg. Chem. 45 (2006) 2055–2060.
[15] (a) S.A. Zubairi, S.M. Ifzal, A. Malik, Inorg. Chim. Acta. 22 (1977) L29–L30;
(b) J.F. Liu, X. Chen, E.B. Wang, Acta. Chim. Sinica. 46 (1988) 1168–1174;
(c) M.R. Antonio, L. Soderholm, G. Jennings, L.C. Francesconi, M. Dankova, J. Bartis, J. Alloys Comp. 275 (1998) 827–830.
[16] R. Contant, R. Thouvenot, Can. J. Chem. 69 (1991) 1498–1506.
[17] L. Spek, PLATON, A Multipurpose Crystallographic Tool, Utrecht University, Utrecht, The Netherlands, 1998.
[18] D.H. Li, S.X. Liu, C.Y. Sun, L.H. Xie, E.B. Wang, N.H. Hu, H.Q. Jia, Inorg. Chem. Commun. 8 (2005) 433–436.
[19] J.F. Cao, S.X. Liu, R.G. Cao, L.H. Xie, Y.H. Ren, C.Y. Gao, L. Xu, Dalton Trans. (2008) 115–120.
[20] D. Brown, D. Altermatt, Acta Crystallogr. Sect. B. 41 (1985) 244–247.
[21] (a) N. Massayuki, A. Yoshihiro, J. Non-Cryst. Solids 197 (1996) 73–78;
(b) Q.H. Xu, L.S. Li, X.S. Liu, R.R. Xu, Chem. Mater. 14 (2002) 549–555.